Langmuir

Invited Feature Article

pubs.acs.org/Langmuir

Periodic Metallic Nanostructures as Plasmonic Chemical Sensors

Chiara Valsecchi and Alexandre G. Brolo*

Department of Chemistry, University of Victoria, P.O. Box 3065, Victoria, BC, Canada

ABSTRACT: Periodic plasmonic nanostructures are being widely studied, optimized, and developed to produce a new generation of low-cost and efficient chemical sensors and biosensors. The extensive variety of nanostructures, interrogation approaches, and setups makes a direct comparison of the reported performance from different sensing platforms a challenging exercise. In this feature Article, the most common parameters used for the evaluation of plasmonic nanostructures will be reviewed, with particular focus on the advances in periodic plasmonic nanostructures. Recent progress in the fabrication methods that allow for the high-volume production of periodic plasmonic sensors at low cost will be described, together with an assessment of the state of the art in terms of periodic structures employed for chemical sensing.

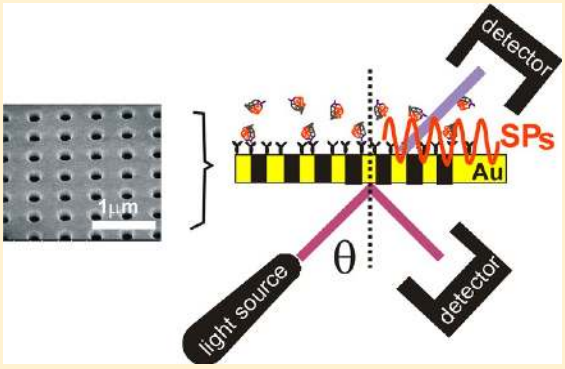

INTRODUCTION

Plasmonic materials, defined as metallic nanostructures that support surface plasmon (SP) oscillations, constitute one of the most explored platforms for chemical sensing. The surface plasmon resonance (SPR) sensitivity to the dielectric environment in the vicinity of the metal surface forms the basis of the sensors.[1] Au, Ag, and Cu are metals that support SP waves in the visible and near-infrared (NIR) range, and their plasmonic materials offer a large range of advantages in the context of chemical sensors, including facile surface chemistry for the immobilization of molecular recognition elements;[2] the possibility of a small (subwavelength) sensing area;[3,4] the potential for massive multiplexing (detection of several different chemical species at the same time);[5] easy integration with microfluidics,[6] leading to small device footprint; and excellent sensitivity. All these favorable properties justify the high research activity aimed at the development of different types of SPR-based sensors. In fact, any architecture that support SPs is a potential chemical sensor, and proof-of-concept molecular detection has been demonstrated for virtually all of them, including thin metal films; metallic nanoparticles, either randomly distributed[7] or single particles;[8] and SP-based waveguides.[9] It is then not surprising that several reviews and books on the subject of plasmonic sensors have been published in the past few years.[1,10−13] The relatively narrow scope of this Feature Article will concern only periodic plasmonic substrates, specifically, periodic arrays of metallic nanoparticles or nanoholes on metal thin films. Figure 1 illustrates a few examples of the variety of arrays of nanoholes and nanoparticles of different shapes, sizes/diameters (d), and periodicities (P) that have been used as chemical sensors. Our main goals are to provide a brief tutorial on plasmonic sensors, including some discussion of the state of the art by covering recent advances in the fabrication of periodic plasmonic structures and their

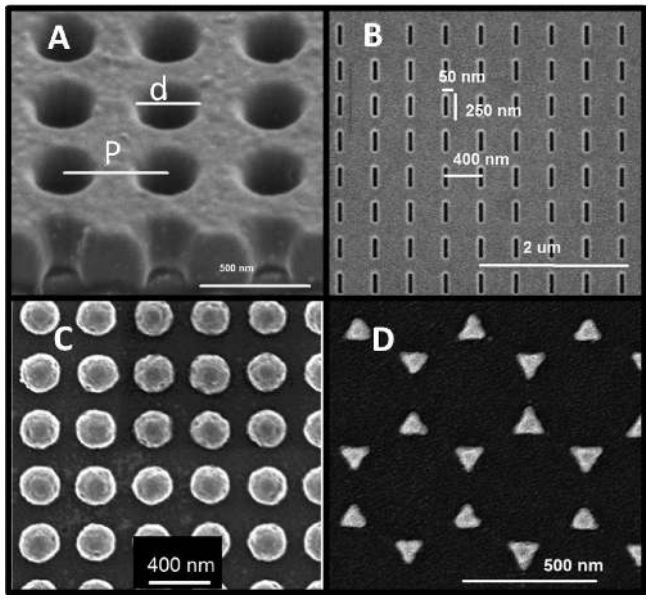

Figure 1. Scanning electron micrographs (SEMs) of different types of periodic plasmonic structures used as chemical sensors. (A) Arrays of circular nanoholes on a 100-nm-thick gold film supported on glass. The distance between the holes is the periodicity, P, and the diameter of the holes (d) is indicated. (B) The same as in A but with rectangular holes instead. The hole dimensions and periodicity are indicated. (C) Square array of circular metallic nanodisks.[13] (D) Arrays of triangularly shaped nanoparticles fabricated using self-assembled nanospheres as templates. [12] Pictures are reproduced with permission from refs 14 and 15.

Received: January 15, 2013
Revised: March 7, 2013
Published: March 14, 2013

   dx.doi.org/10.1021/la400085r | *Langmuir* 2013, 29, 5638−5649

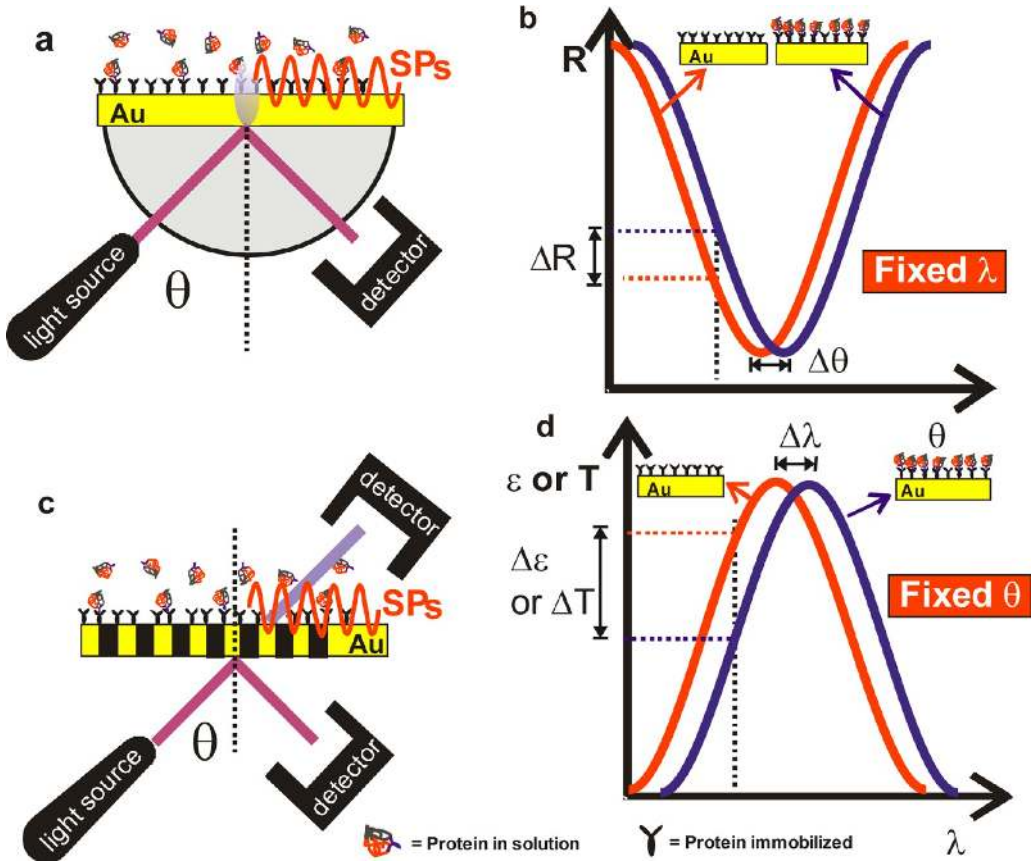

Figure 2. Coupling schemes for the generation of SPs. (a) Kretschmann–Raether arrangement (prism coupling); (b) schematic of reflectance curves, before and after adsorption, obtained from a prism-coupling experiment; (c) grating coupling, the usual arrangement used for chemical sensing with periodic plasmonic structures; (d) schematic of extinction or transmission measurements that are typically obtained from grating-coupling experiments.

evaluation as chemical sensors and a brief comparison of the performance from different platforms.

Although plasmonic effects also form the basis for a series of surface-enhanced spectroscopic methods such as surface-enhanced Raman scattering (SERS),[16] this article will concentrate only on refractometric-based SPR.

SPR SENSING: BASIC CONCEPTS

SPs cannot be created on a smooth metal surface by direct optical excitation.[1] The reason is that the SP momentum is larger than that of a free photon, and direct light-to-SP conversion is forbidden. Therefore, special coupling schemes, as depicted in Figure 2, need to be devised to allow for SP generation.

The most common configuration for SP-based sensing is the prism coupling proposed by Kretschmann and Raether (Figure 2a).[17] In this case, the evanescent field from the totally reflected light from the prism side extends through a thin metal film (about 50 nm) to launch SPs on the other side of the film (Figure 2a). In a typical experiment, a (p-polarized) monochromatic light source is used and the intensity of the light reflected from the prism side (reflectivity (R)) is measured at different angles of incidence (θ). An R versus θ plot, schematic shown in Figure 2b, will present a minimum at the angle where the incident light is absorbed to generate SPs (SPR angle; θ_{SPR}). The position of θ_{SPR} is dependent on the effective refractive index at the metal surface. The adsorption of molecular species at the top metal surface, as illustrated in Figure 2a, changes the conditions for SP generation (by changing the refractive index adjacent to the metal surface), provoking a shift in the θ_{SPR} position in the reflectivity curve (Figure 2b). The quantity $\Delta\theta$ is the measured response of the sensor in this case (angular interrogation). Because plasmonic sensing is a refractometric measurement, the platforms are not inherently able to recognize particular chemical species of interest. The selectivity of the sensor is imparted by the appropriated surface modification.[2] In the generic example of Figure 2, the metal surfaces are modified by a capture target that recognizes a specific protein in solution. Another common experimental mode in Kretschmann–Raether-based SPR consists of maintaining a constant angle of incidence for the monochromatic light (closer to the minimum) and monitoring the reflectivity changes (ΔR) during adsorption (binding). This fixed angle arrangement, indicated in a schematic plot in Figure 2b (also known as an intensity interrogation mode), is widely used in biomedical research because it allows the determination of real-time binding kinetics.[1] The Kretschmann–Raether configuration SPR is the most common arrangement for studying biomolecular interactions and affinities that is available commercially (e.g., www.Biacore.com).

Another approach is to generate SPs by grating coupling, which employs metal films with subwavelength periodic corrugations, as illustrated in Figure 2c. These corrugations can be periodic arrays of either metallic nanoparticles supported in a dielectric substrate or subwavelength holes (nanoholes) perforated in a metal thin film. These are typical periodic

dx.doi.org/10.1021/la400085r | Langmuir 2013, 29, 5638–5649

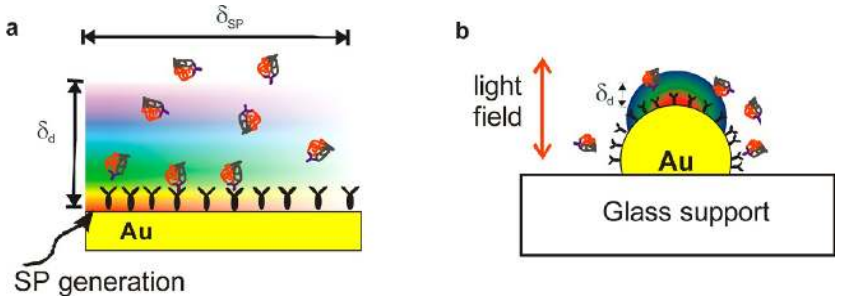

Figure 3. Illustration of characteristic lengths of SPs. (a) PSP case: an SP wave is generated and it propagates parallel to the surface to a distance of δ_{SP}. The wave propagation is attenuated by the intrinsic metallic absorption and others losses channel, such as surface roughness and defects. The color-coded diagram illustrates an exponential decrease in the SP field from the most intense value at the surface (red) toward the dielectric (violet corresponds to $^1/_e$ of the maximum field strength). The decay length of the field is δ_d. (b) Free electrons in metal nanoparticles can be collective driven by an incident light field (diameter smaller than the incident wavelength), generating LSPs. The color code shows a schematic of the field-strength decay length (from red (maximum field) to blue ($^1/_e$ of the maximum field strength)).

plasmonic structures, with a few examples shown in Figure 1, and they constitute the focus of this Feature Article.

The geometric characteristics of the structures (type of corrugation (particles or holes), shape, and periodicity[18]) can be tailored to control the characteristics (resonance energy) of the SPs. As illustrated in Figure 2c, grating-coupled SPR can be realized in either reflection or transmission mode.[1,8] In the case of periodic arrays of nanoparticles, the most common measured quantities are the extinction parameters (light absorption + scattering) of the substrate (ε),[8] whereas in the case of nanohole arrays the SPs allow enhanced light transmission (T) at particular wavelengths, a phenomenon known as extraordinary optical transmission (EOT).[19] Similar to the Kretschmann−Raether case, either the maximum in extinction or the maximum in transmission will shift when the dielectric conditions at the metal interface are altered by molecular adsorption. Although measurements of θ_{SPR} can also be realized in grating-coupling SPR using monochromatic radiation (angular interrogation, as in Figure 2b), in most cases reported in the literature the periodic plasmonic structures are illuminated with white light at a fixed angle (normal incidence is the most common) and peaks in either extinction or transmission reveal the resonance conditions (wavelength interrogation mode, as represented schematically in Figure 2d).[6] As indicated in Figure 2d, intensity interrogation in the form of changes in light intensity from a monochromatic source ($\Delta\varepsilon$ or ΔT) at a fixed angle can also be used to follow the binding kinetics in periodic plasmonic nanostructures.

SPs can be broadly classified according to the characteristics of their electromagnetic field. They are the propagating surface plasmons (PSPs) and the localized surface plasmons (LSPs). The main characteristic lengths of PSPs are represented schematically in Figure 3a. The SP field intensity is maximum at the metal surface, but it evanescently decays toward the dielectric with a decay length of δ_d. Typically, δ_d values for PSPs are on the order of half of the resonance wavelength for structures excited in the visible range. The PSP waves also travel parallel to the surface with a propagation length of δ_{SP}. The values of δ_{SP} depend on the loss channels that affect the propagation at particular excitation energies, but generally δ_{SP} is between 5 and 500 μm for experiments in the visible and near IR.[20] The δ_{SP} value determines the minimum size of a PSP sensing element. PSPs are present in both prism- and grating-generated SPs, as illustrated in Figure 2. An example of LSPs, shown in Figure 3b, is from the excitation of electronic oscillations in an Au nanoparticle immobilized on a glass surface. Under those conditions (diameter ≪ wavelength), the momentum conservation requirements are relaxed and SPs can be directly excited. Figure 3b shows a condition where the resonant light field induces the displacement of the free electron cloud in an Au nanoparticle, generating a dipolar response. The local field generated by the SP excitation is confined around the nanoparticle (no propagation) and also decays exponentially toward the dielectric with a typical length of δ_d. In the case of LSPR, however, the δ_d value is only on the order of a few tens of nanometers (depending on the type of metal and nanoparticle shape and size).[21] The SP field in the LSPR case is then more confined to the metal surface than in the case of PSPs.

In the context of periodic plasmonic structures, both PSPs and LSPR resonances might play a role in a particular system. Grating-generated SPs have defined δ_{SP} values and show an angular dependence that is characteristic of PSPs. However, SP fields can be localized in shaped elements of the periodic structure.

FABRICATION OF PERIODIC PLASMONIC STRUCTURES

Research on periodic plasmonic structures and grating-based SPR sensing has increased drastically in the past few years. The increased activity in this area started in the late 1990s, and it is correlated to the increased availability of top-down specialized nanofabrication methods such as focused ion beam (FIB) milling and electron beam (e-beam) lithography (EBL). The FIB method consists simply of bombarding the (metal) sample with gallium ions to sculpt any desired pattern.[22] Electron beam lithography (EBL) uses electrons (rather than light in conventional photolithography) to write directly (maskless) and sensitize a resist (normally poly(methyl methacrylate), PMMA).[23] The patterns can then be developed and the sample can be processed using steps that are well established in the microelectronics industry. Both FIB and EBL allows precise control of the shape and size of the structures with an ultimate resolution of only a few nanometers.[23] These methods are then excellent for the systematic evaluation of geometrical parameters and the fundamental understanding of their effect on the plasmonic properties of periodic structures. However, both FIB and EBL are serial fabrication methods that require costly specialized instrumentation. Moreover, they are not suitable for large-area patterning, and the typical sensing areas obtained using these methods are on the order of 30 × 30 μm^2

dx.doi.org/10.1021/la400085r | Langmuir 2013, 29, 5638−5649

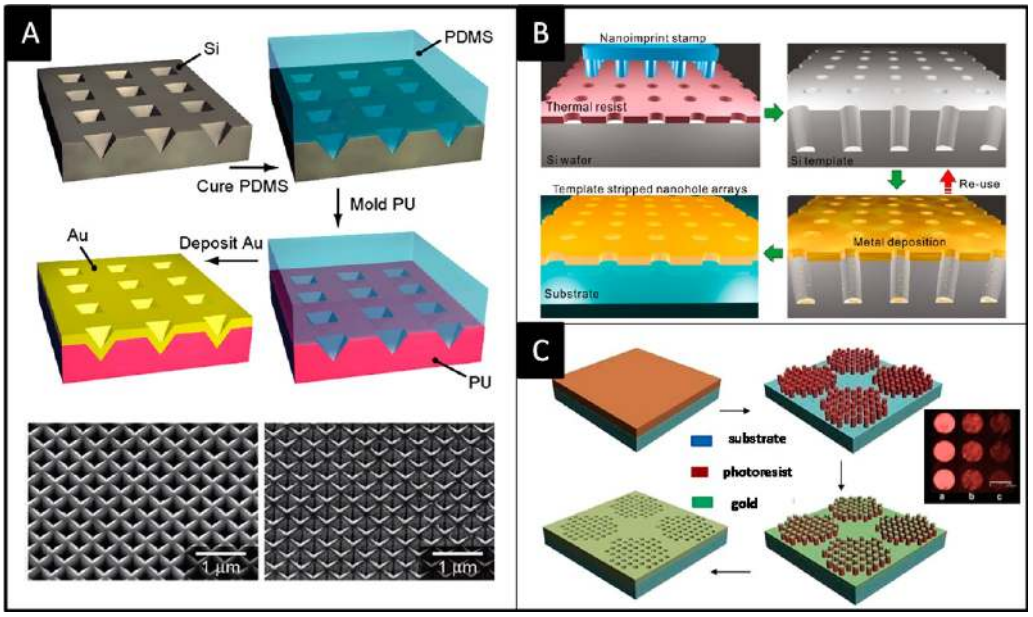

Figure 4. Examples of methods that allow the fabrication of large-area periodic plasmonic structures: (A) periodic plasmonic structures are generated from metal deposited on polyurethane (PU) replicas from a Si template; [30] (B) template stripping method where the plasmonic structure is generated from metal deposited on a Si master;[31] and (C) interference lithography to fabricated nanohole arrays, followed by regular photolithography to define sensing "patches" suitable for multiplexing detection.[33] Images are reproduced with permission from refs 31−33.

for FIB and 100 × 100 μm^2 for EBL. Although improvements in beam focus, directionality, and other aspects allowed the patterning of 1 cm^2 by EBL,[24] these methodologies are clearly too slow and expensive to be considered as viable tools for the mass fabrication of periodic plasmonic sensors.

Recently, the fabrication focus of periodic metallic structures has changed toward the implementation of methods for large-area patterning that are suitable for mass production.[25−27] These approaches are more appropriate for the possible commercialization of the new generation of plasmonic sensors based on periodic structures. Many techniques for large-area patterning have been reported, including soft lithography,[28] nanoimprinting,[29] and templating using either block copolymers or polystyrene nanospheres.[30]

Figure 4 shows three examples of large-area patterning that fulfill the demands of low cost and high throughput required for the mass production of sensor devices. Figure 4A illustrates an approach where a poly(dimethylsiloxane) (PDMS) stamp, obtained from a master structure fabricated in silicon, was used to mold a pattern in UV -curable polyurethane (PU) matrices. The PU substrate was then coated with a metal film, reproducing the original pattern of the master.[31]

Figure 4B demonstrates the fabrication of large-area nanoaperture arrays by a template-stripping method.[32] A nanoimprint stamp was first generated from an EBL-fabricated master. The stamp was used to transfer a pattern to a silicon substrate. A metal film was then evaporated onto the patterned silicon, as illustrated in Figure 4B. In the last step, an epoxy resin was applied to the metal film, and because the metal interaction to the epoxy is stronger than with the silicon substrate, the whole structure was easily peeled off of the silicon master.[32] The overwhelming advantage of this method is that the smoothness of the silicon substrate is imprinted on the metallic surface of the sensor, allowing for longer PSP propagation and sharper plasmonic resonances. The PDMS stamp in Figure 4A and the Si template in Figure 4B are reusable, allowing the fabrication of hundreds of metallic periodic structures from an original master with high fidelity. Figure 4C illustrates an example of periodic nanohole array patches fabricated in gold thin films by interference (or holographic) lithography (IL).[33] Photolithography is widely used in the microelectronics industry to generate patterned surfaces and devices. However, plasmonic sensors require metallic features below 200 nm, and this size range is achievable only with conventional lithography in the UV region. A low-cost benchtop UV photolithography system has been recently reported,[34] and the combination of UV with near-field optics[35] allowed spatial resolutions that rival the EBL method. However, the use of short wavelengths and near-field probes requires costly specialized optics and infrastructure. The IL method, however, can be used for the fabrication of periodic (1D, 2D, or 3D) nanostructures using visible radiation.[32,33,35,36] The process involves the combination of laser beams (from two or more arms from the same beam) on the surface of a substrate coated with a photoresist, generating a predetermined interference pattern that is transferred to the photoresist. Further exposure through a micropatterned mask using a regular UV lamp led to a structure of patches, illustrated in Figure 4C, that are ideal for multiplexing biosensing (simultaneous detection of different proteins from different patches). The metal deposition and lift-off steps that follow the IL writing (and the subsequent regular photolithography in Figure 4C) are standards in any fabrication laboratory. Periodic plasmonic structures fabricated by IL were compared to equivalent FIB-fabricated substrates and showed similar plasmonic sensing performance.[37] The IL technique is quick, easy, and takes advantage of the fabrication know how already established in the microelectronics industry, being a good candidate for the mass-scale production of periodic plasmonic geometries.

dx.doi.org/10.1021/la400085r | *Langmuir* 2013, 29, 5638−5649

PERFORMANCE OF PLASMONIC SENSORS

Different types of periodic plasmonic biosensors, fabricated by diverse methods, have been reported in the past few years.[26,31−33,38] However, it is sometimes difficult to compare the sensing characteristics of different platforms because of the various ways that the performance of the sensors are evaluated and reported. However, the performance characteristics of commercially available SPR devices, based on the Kretschmann−Raether configuration, are widely used in the field as benchmarks. The general objective in the area then is to produce platforms that can outperform the commercial state of the art and/or provide additional advantages in terms of analysis speed, device miniaturization, and multiplexing. Before comparing a variety of periodic plasmonic sensors from different groups, a brief description of the main sensor performance characteristics will be introduced.

Several contributions participate in the outcome of a sensing platform, varying from the design and quality of the fabricated periodic structure to the method used for the detection of the sensor response, including the overall setup instrumentation and surface chemistry. An understanding of these contributions is important in comparing sensors from different laboratories.

The simplest quantitative performance parameter of a plasmonic sensor is the sensitivity to bulk refractive index changes (bulk sensitivity, S_b). In a typical experiment (for instance, the experimental arrangement illustrated in Figure 2c), the periodic plasmonic nanostructure is exposed to liquids with different refractive indexes, and shifts in the SPR (as illustrated in Figure 2d) are recorded. The bulk sensitivity (S_b) is the slope of the plot between the changes in the measured quantity ($\Delta\theta$, $\Delta\lambda$, ΔT) versus the refractive index of the liquids. It is important to point out that the sensitivity of the SPR sensor is wavelength-dependent; therefore, the direct comparison of performance needs to be considered in the same range of wavelength. The bulk sensitivities from arrays of either metallic nanoparticles or nanoholes are generally between 300 and 600 nm/RIU in the visible range.[26,33,36,39] A comparison of S_b behavior for both grating- and prism-coupled SPR systems has been reported. In principle, grating-based SPR sensors are less sensitive to bulk refractive index variations then prism-based sensors in wavelength interrogation mode (measurement of $\Delta\lambda$, as in Figure 2d). However, their S_b values are comparable in angular interrogation mode (Figure 2b).[40]

In most applications, however, plasmonic platforms are required the detection of surface binding events rather than bulk refractive indexes, and S_b is not the best metric for surface sensing performance. The differences between bulk (S_b) and surface sensitivity (S_s) will be discussed next.

Figure 5 illustrates the evanescent nature of the intensity (E^2) of the SP field, which decays exponentially from a maximum value at the metal surface toward the solution (δ_d is roughly half of the exciting wavelength for the PSP case).[41] The characteristics of the SP mode depend on the refractive index within this decaying field. Figure 5a illustrates the simplest case: without molecular adsorption. This situation occurs when the sensitivity of the SPR platform is tested by exposing the metal surface to liquids of different refractive indexes (S_b case). Notice that eventual differences in the dielectric properties from the structure of the molecules of the liquid in the double-layer region (structured solvent layer adjacent to the metal surface) are not considered in this model. In that case (Figure 5a), the refractive index inside the SP field is homogeneous and

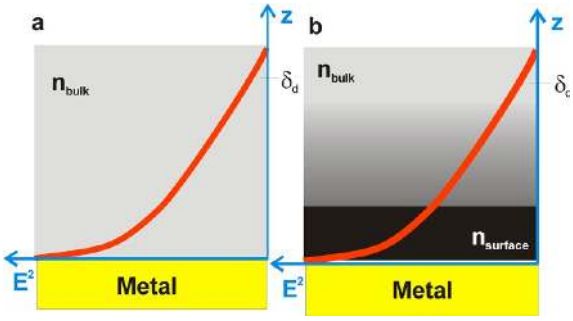

Figure 5. Schematic of the decay field profile (field intensity (E^2) variation from the surface toward the bulk − z axis): (a) in the absence of adsorbates and (b) in the presence of adsorbates. n_{bulk} and $n_{surface}$ correspond to the refractive index of the bulk liquid and the adsorbed layer, respectively.

the sensor responds to bulk refractive index changes. Figure 5b shows the case where a layer of adsorbate is formed. As observed in Figure 5b, the binding of species to the metal is probed by only a small part, although the most intense part, of the SP field. Figure 5b also shows that the SP field probes the bulk index and the index gradient (formed, for instance, by loosely adsorbed species or by the diffusion layer) between the surface and the bulk. The index gradient contribution can be eliminated by simply flushing the solution with the solvent (electrolyte) prior to the measurement. In other words, in a typical surface sensing experiment (such as in biosensing, for instance), a baseline is established with an appropriate electrolyte that does not contain species that adsorb to the surface (for instance, phosphate-buffered saline (PBS) solution), a situation akin to Figure 5a. Then a solution containing the analyte is introduced, and the conditions described in Figure 5b are established. After a certain amount of time, the initial electrolyte is again introduced into the system, taking away the unbound species and, ideally, leaving only a layer of the adsorbate attached to the surface. The sensor response in the presence of adsorbates will depend on the effective refractive index inside the SP field. In a first approximation, this effective refractive index can be estimated using a weighted average within the exponential SP decay.[41]

In terms of surface sensors, the useful performance parameter that allows for a comparison between different platforms is then the surface sensitivity (S_s), defined as the sensor response to a determined number of molecules adsorbed to the surface. Parameters such as the surface coverage, given in terms of either the number of molecule per mm^2 or the mass per mm^2, are then required to evaluate S_s values. This type of information can be obtained by independent measurements. For instance, QCM (quartz crystal microbalance) experiments can be used to obtain the mass of adsorbates. Other approaches have also been reported to evaluate S_s experimentally. For example, the performance of the commercial system from Biacore was evaluated by comparing the response of their SPR system after protein adsorption experiments to the surface coverage measured by scintillography using ^{14}C-labeled proteins.[42] An average unit response value per surface coverage was obtained. Interestingly, the instrument response per surface coverage (in pg/mm^2) was the same for proteins of different molar masses because the refractive index of protein films does not depend strongly on the nature of the protein.[41]

The surface sensitivity can also be reported in terms of sensor response to a certain adlayer thickness (S_{st}). For

dx.doi.org/10.1021/la400085r | Langmuir 2013, 29, 5638−5649

wavelength interrogation, S_{st} is given in nm (of wavelength shift)/nm (of adlayer thickness). Parameters available in the literature for the density and thickness of most common self-assembled monolayers (SAMs) and polymeric materials are then used for the estimation of the adlayer thickness at the metal surface. In particular, the layer-by-layer deposition of positively and negatively charged polymers, such as polyallylamine (PAA) and poly(sodium styrene sulfonate) (PSS), respectively, have been mostly used.[43] In this case, relative homogeneous surface layers of the polymers with defined thickness can be formed rapidly by electrostatic interactions. The structures can be independently evaluated by ellipsometry to closely relate the SPR shift with the layer thickness. The relative consistency of the layer-by-layer growth allows this method to be used to estimate the value of δ_d.

The sensitivity can also be expressed in terms of the sensor response to changes in the analyte concentration in solution (concentration sensitivity (S_c)). S_c values are obviously dependent on the type of analyte and on the strength of the molecular interaction with the surface layer, given by the adsorption constant. Although S_c is sometimes reported in SPR sensor evaluation involving periodic plasmonic structures, the quantity is not general enough to be useful for the comparison between different platforms.

Another very important aspect that can be obtained from Figure 5b is that plasmonic devices with more surface-confined SP fields (smaller δ_d values) should present better S_s values. Notice that the adsorbate layer in Figure 5b overlaps with part of the SP field. The overlap should be larger when δ_d is smaller. In fact, there is theoretical and experimental evidence (for wavelength interrogation) in the literature demonstrating this assumption. For instance, although LSPR platforms have bulk sensitivities that are an order of magnitude smaller than those of PSP devices, their surface sensitivities are equivalent as a result of the more surface-confined nature of the LSPR.[8,44] It is important to point out, however, that because the evanescent decay field is about only 5% of the incident wavelength for LSPR devices, they can only be efficient as surface sensors (or biosensors) if the surface-modification layer (immobilized species that confer the selectivity to the sensor) does not exceed about 20 nm.[45]

Although most of the papers on new types of periodic plasmonic structures as chemical sensors report some sort of sensitivity (bulk or surface), there are other parameters that need to be considered in the comparison of different platforms, including the spectral shape and the noise in the detection system.

The spectral shape is taken into consideration by calculating a figure of merit (FoM) according to

$$\mathrm{FoM} = \frac{S_b}{\mathrm{fwhm}} \tag{1}$$

where S_b is the bulk sensitivity (given, for instance, in nm/RIU when $\Delta\lambda$ is monitored (wavelength interrogation)) and fwhm is the full-width at half-maximum of the SP resonance being considered. The fwhm, in fact, is related to the SP lifetime (or propagation length, δ_{SP}, in the case of PSPs), which generally controls the sharpness of the peak. The FoM is probably the most popular metric for comparing the performance of plasmonic platforms.[46] Again, it is important to point out that the FoM is wavelength-dependent, and a comparison between sensors needs to take that into consideration.[11] The concept of FoM was recently expanded by taking into consideration the physical characteristics of the device.[47]

The diffraction characteristics of periodic plasmonic structures allow the occurrence of asymmetric sharp peaks due to Fano resonances. This feature arises from the interference between resonant and nonresonant channels.[48] Intrinsically, the Fano feature is more sensitive to a change in the dielectric environment, and an ∼2-fold improvement (compared to typical values from grating-based SPR) in bulk sensitivity (S_b) has already been reported.[49] Moreover, the sharpness of the peak (smaller value for the fwhm) also contributes to a larger FoM value according to eq 1. Periodic plasmonic sensors based on Fano resonance have been shown to present performance comparable to that of commercial state of the art.[50]

The use of only the FoM to compare plasmonic platforms, however, does not take into consideration instrument factors (it is considered that the fwhm is not limited by the spectral resolution of the instrumentation), such as the detection method, setup configuration, and overall instrumentation performance and noise. The development of SPR platforms is generally driven toward the detection of the smallest concentration of analytes, including proteins, antibodies, cancer markers, and DNA/RNA base pairs, to achieve certain biomedical goals such as to determine genetic mutations or for the early diagnosis of illnesses. In addition, the sizes of the most common SPR analytes are on the order of 1 to 2 nm. All of this means that that the goal is to detect a small number of surface binding events involving small molecules that lead to a small perturbation within the sensing volume of the SP field. In this sense, the concepts of sensor resolution (res) and limit of detection (LOD) are then the most appropriate parameters for determining the overall efficiency of a plasmonic structure such as chemical sensors. In that sense, these are the best quantitative parameters for comparing the performance of different platforms. The term "resolution" in SPR means the smallest detectable change in refractive index. The LOD has a connotation familiar to analytical chemists, and it is defined as the minimum variation of the measured quantity that the sensor can detect with reasonable certainty (normally taken as 3 or 5 times the standard deviation of the signal).[1] The resolution is then reported in RIU (refractive index units), and the LOD is reported either in surface coverage units (pg/mm^2) or in terms of the minimum concentration detectable for a particular analyte. Experimentally, the resolution (res) is easier to determine because it does not require any information about the surface concentration and it does not depend on the chemical nature of adsorbates. res is obtained from the noise in the detector output (for instance, the noise in the determination of a wavelength shift in nanometers), σ_{so}, and the bulk sensitivity (S_b in nm/RIU) according to

$$\mathrm{res} = \frac{\sigma_{so}}{S_b} \tag{2}$$

Improving res can then be achieved by reducing noise and improving the sensitivity of the plasmonic platform. There are at least three types of instrument noise common in plasmonic sensors: (1) the noise derived from the fluctuation of the light source, which is proportional to its intensity; (2) the shot noise, from Poisson statistics of the photon flux, which is proportional to the square root of the light intensity; and (3) the read-out noise, which relates to all the electrical conversions and propagations of the signal. The role of each one of these types

dx.doi.org/10.1021/la400085r | Langmuir 2013, 29, 5638−5649

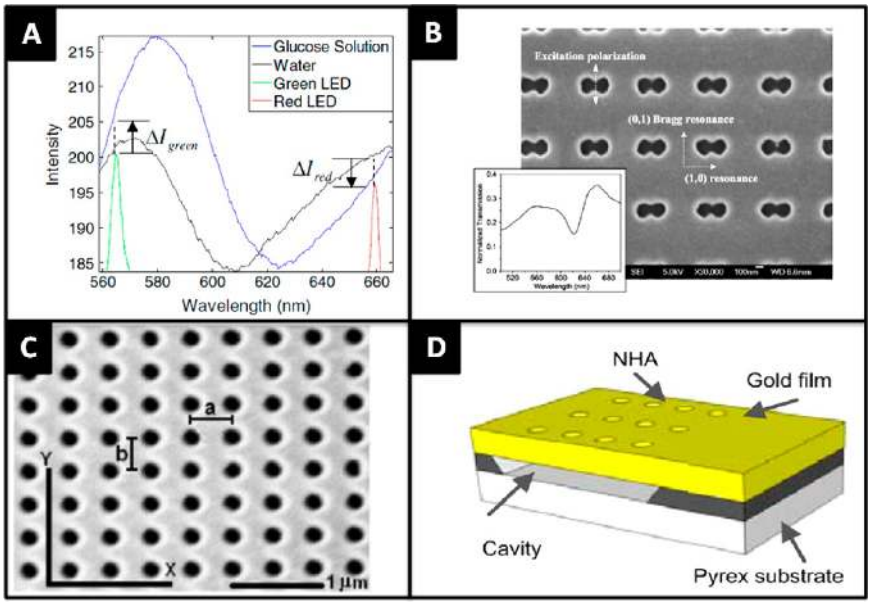

Figure 6. Examples of approaches used to improve the performance of periodic plasmonic structures. (A) A dual-wavelength interrogation scheme is used to create a reference channel.[51] (B) Arrays of double holes that present better bulk sensitivity than array of circular holes due to the LSPR from the apexes.[39] (C) Array of nanoholes with different periodicities in the *x* and *y* directions allow different resonances to be accessed by polarization selection. This approach can also lead to a polarization-sensitive reference channel.[57] (D) Nanofabrication is used to etch the glass supporting an array of nanoholes.[58] This approach allows the solution to access the space under the array, leading to better refractive index matching between both sides of the gold interface. Narrower SPR is the result of the matching refractive indexes. Images are reproduced with permission from refs 39, 51, 57, and 58.

of noise in the SPR resolution has been discussed elsewhere.[1] Stable light sources, temperature control, vibration-isolated tables, reference channels, and high-end detectors and cameras are common approaches to improving noise levels. Figure 6A, for instance, illustrates a dual-wavelength approach to generating an in situ reference channel.[51] The two colors are chosen to be on each side of the resonance peak such that the intensity at one channel decreases while that at the other increases during a peak shift. The signal-to-noise ratio (SNR) is improved because the difference between the red and green variations (indicated in the figure) eliminates spurious artifacts.

Data treatment algorithms can also be used to decrease the variation in the determination of the system response. For instance, a simple fit of the SPR peak, instead of using the noisier raw data, allow for a better localization of the resonance. More elaborate statistical approaches have been implemented to provide a more robust monitoring of spectral changes. The centroid method,[52] for instance, follows the changes in the geometrical center of a portion of the SPR peak with a high degree of accuracy. Other protocols use the concept of an integrated response, where changes in the whole spectrum, rather than a single-point peak shift, are evaluated.[43,53] The integrated response method was proven to increase the signal-to-noise ratio significantly.

The majority of the effort in plasmonic sensor research, however, is centered mostly on improving sensitivity (although, as shown in eqs 1 and 2, the sensitivity is not the only variable that determines the performance (resolution) of the sensor). Particularly for periodic plasmonic structures (arrays of metallic nanoparticles on glass, subwavelength holes on metal films, or even some combinations of these structures), the parameter space to be explored includes the thickness of the metal layer,[54] the distance between the elements of the arrays (periodicity), and the shape of the individual elements. Figure 6B shows an example of improved sensitivity achieved by changing the shape of the nanoholes. In that case, overlapping double-hole arrays were used instead of single circular apertures.[39] The reported improvement in sensitivity was attributed to LSPR contributions at the double-hole apexes. The shape effect in periodic structures can also contribute to improvements in surface sensitivity because their LSPR characteristics present lower δ_d values. The shape effect on the sensitivity of the sensors has been explored by using elliptical holes, tiny slits, and squares cavities. The same sort of shape effect has been observed for arrays of nanoparticles.[55] Similar to nanohole structures, the more localized sensing field observed for sharper features correlates to better overall performance in periodic arrays of nanoparticles. For instance, the bulk sensitivity decreases from arrays of nanorods to arrays of triangularly shaped nanoparticles to arrays of nanodisks. Also, increasing the in-plane width and the out-of-plane height of nanoparticles in the arrays might influence their sensitivities. For instance, upon decreasing the height by 70%, a sensitivity boost of almost 350% was found for arrays of triangular nanoparticles.[8] The use of arrays of double particles (disks), separated by small (less than 30 nm) gap distances, also leads to better sensitivity because of near-field coupling effects.[56]

The use of anisotropic elements in periodic plasmonic structures, as shown in Figure 6B, opens up the possibility of polarization selectivity to improve the signal-to-noise ratio (SNR). As can be seen in Figure 6B, the relevant LSPR for that structure is excited only when the polarization of the excitation is parallel to the apexes.[39] Therefore, excitation polarized perpendicular to the apexes offer a reference channel that can be used to eliminate noise.

A similar polarization-selective approach was explored in the structure presented in Figure 6C.[57] In this case, the array presented different periodicities for each direction (*x* and *y*,

dx.doi.org/10.1021/la400085r | *Langmuir* 2013, 29, 5638−5649

Table 1. Summary of the Performance of Selected Periodic Nanohole Arrays

SPR detection scheme	sample/fabrication	performance	(comments)	ref
spectral interrogation	square arrays of circular nanoholes on gold/FIB	S_b = 400 nm/RIU S_c = 16 nm/(mg/mL)	(streptavidin−biotin)	6
spectral interrogation	square arrays of circular nanoholes on silver/template stripping	S_b = 450 mn RIU^{-1}; res = 2 × 10^{-5} RIU		26
spectral interrogation intensity interrogation	square arrays of circular nanoholes on au/interference lithography	S_b = 271 nm/RIU S_c = 15%/(μg/mL) FoM = 11.7	(streptavidin−biotin)	33
spectral interrogation	square arrays of circular nanoholes on gold/soft lithography	S_b = 313 nm/RIU; FoM = 23.3		36
spectral interrogation	square arrays of double nanoholes on gold/FIB	S_b =600 nm/RIU S_{st} = 6 nm/1.6nm S_c = 3 nm/0.2%	(thiol SAM) (BSA solutions)	39
intensity interrogation	rectangular array of circular nanoholes on gold/FIB	res = 6.4 × 10^{-6} RIU		59
phase interrogation	square arrays of circular nanoholes on gold/FIB	res = 2.9 × 10^{-7} RIU		62
intensity interrogation	square arrays of circular nanoholes on gold/FIB	S_{st} = 3.5%/nm S_b = 16 600%/RIU	(thiol SAM)	5

Table 2. Summary of the Performance of Selected Periodic Arrays of Nanoparticles

SPR detection scheme	sample/fabrication	performance	(comments)	ref.
spectral interrogation	hexagonal array of triangular gold nanoparticles/nanosphere lithography	S_c = 0.3 nm/(pg/mL)	(serum p53 protein)	14
spectral interrogation	copper particles deposited on silica nanoparticles/e-beam evaporation	S_b = 67.8 nm/RIU LOD = 10 fM	(DNA)	63
spectral interrogation	hexagonal array of spherical gold nanoparticles/ block copolymer lithography	S_b = 47 nm/ RIU S_c = 0.4nm/ (ng/mL)	(PSA antibody)	38
spectral interrogation	hexagonal array of triangular gold nanoparticles embedded in glass/nanosphere lithography	S_{st} = 1.36 nm/nm	(SAM polymers)	64
spectral interrogation	silver nanoparticles deposited on nanowells/ nanosphere lithography	S_b = 538 nm/RIU FoM = 14.5		65
spectral interrogation	square arrays of gold nanodots/Stencil lithography	S_b = 179 nm/RIU S_c = 10 nm/μM	(streptavidin−biotin)	44
wavelength interrogation	square arrays of Ag nanodisks/ EBL	S_b = 354 nm/RIU FoM = 2.81		66

defined in Figure 6C). Because the PSP will be excited in the polarization direction, light polarized parallel to the x axis will produce a resonance compatible to the periodicity in that direction. However, the position of the resonance peak will be at a different position when the polarization of the excitation light is parallel to the y axis.[59] The differential SPR shift from both polarizations can then be obtained and compared to eliminate common noise. Another fabrication approach to improved sensor performance, illustrated in Figure 6D, consists of providing better matching between the refractive indexes at the top and at the bottom of the sensing surface.[58] An array of nanoholes in a gold film supported in glass, for instance, will have a refractive index mismatch between the gold−glass (n≈1.5) and the gold−solution ($n \approx 1.33$) interfaces. This asymmetric structure presents more losses, broader resonances, and less sensitivity.[1,60] The matching of indexes below the sensing surface with the liquid or solution that is being tested, as shown in Figure 6D, increases the PSP propagation length, increasing the interaction with the environment being sensed, leading to better sensitivity.[58] The refractive index matching in Figure 6D is achieved through the etching of the volume under the gold film, generating a cavity that is filled with the sensing solution. Other approaches involve depositing the gold film on polymeric materials, such as fluoropolymers (Teflon and Cytop), that have refractive indexes close to those of typical aqueous solutions.[61]

The sensitivity can also be enhanced by special measurement configurations, such as phase-sensitive detection.[62] The change in phase that accompanies the SPR is very steep, allowing a larger response even for a very small surface perturbation, such as the adsorption of a small number of molecules. However, the better performance in this case is traded off by the more complex modulation optics and electronics required for the phase measurements. Dark-field microscopy is another approach that leads to better performance. The collection at a low angle of light scattered from metallic particles arranged in periodic arrays provides a better contrast with the background and minimizes the noise from the excitation source.

COMPARING THE PERFORMANCE OF PERIODIC PLASMONIC PLATFORMS

Now that the basic concepts of SPR and the main performance evaluation characteristics have been introduced together with the recent advances in the fabrication of periodic plasmonic structures, we are ready to present a brief survey of some of the plasmonic platforms that have been reported in the past few years.

dx.doi.org/10.1021/la400085r | Langmuir 2013, 29, 5638−5649

Tables 1 and 2 present a collection of periodic plasmonic platforms, nanoholes, and nanoparticle arrays and their associated reported performance parameters. Is it again important to mention that the performance of the sensors is dependent on other variables, such as the wavelength range of the measurements, the diffraction order of the gratings, and the surface chemistry and nature of the analytes. The data summarized in Tables 1 and 2 were from experiments in the visible light and near-IR range and consider only the lowest (first) order of diffraction. Plasmonic sensors that explore Fano resonances were not included. Tables 1 and 2 are not intended to be comprehensive; the objective is only to present an arbitrary selection of periodic plasmonic sensors reported from different groups for a general comparison.

As discussed earlier, the Krestchmann−Raether SPR configuration provides a performance gold standard because it is a well-established technology that is widely used mainly in biomedical research. The ultimate resolution achieved by a state-of-the-art system from Biacore (www.Biacore.com) is reported to be $\sim 10^{-7}$ RIU, and the typical LOD is below 1 pg/mm^2. These are the limits that are expected to be matched (or overcome) by the periodic plasmonic platforms.

Although the typical bulk sensitivity for periodic plasmonic arrays in spectral interrogation generally lies below 1000 nm/RIU,[25,32,35,38,67] several research groups have reported a performance for periodic plasmonic structures that rivals the commercial implementation of SPR.[5,50,67] Intensity interrogation mode and phase change monitoring, in particular, have been shown to reach resolutions of between 10^{-6} and 10^{-7} RIU.

Nanoparticles are widely used in SPR biosensing with periodic structures as detection "enhancers" in sandwich-type assays.[68] Examples of some organized arrays of nanoparticles are listed in Table 2, and their performance in terms of surface sensing is comparable to that of nanohole arrays. Examples of excellent achievements in terms of the determination of low concentrations of bioanalytes from solutions are from the work of Lee et al.[63] and Luo et al.[14] The former detected 10 fM DNA filaments in solution, and the latter were able to measure the binding from 60 pg/mL solutions of p53 antibody from the serum of cancer patients.

In general, periodic plasmonic platforms offer additional advantages over commercial (Kretschmann−Raether-based) SPR systems on top of the quantifiable sensing performance parameters (sensitivity, resolution, and LOD) presented in Tables 1 and 2. For instance, although imaging SPR systems for prism-based SPR are commercially available, allowing the simultaneous detection of several binding events from different spots on the surface (multiplexing), the angular interrogation arrangement (required in prism-based SPR) yields distorted (tilted) images that limit the spatial resolution. Easier multiplexing in miniaturized devices can be achieved using periodic plasmonic structures because the SPR excitation can be realized at normal illumination.[5,33] Normal excitation allows the use of optimized imaging optics, including high-numerical-aperture objectives, improving light collection and reducing noise. Moreover, the simplified collinear optical arrangement (normally used for periodic plasmonic structures) is best suited for their implementation as detection elements in lab-on-a-chip devices. For instance, miniaturized readers have been reported for arrays of nanoholes integrated with microfluidic channels.[69] In fact, the straightforward microfluidic integration constitutes a major drive toward the development of periodic plasmonic structures for chemical sensing applications. Recently, the ultimate plasmonic−fluidic integration was achieved using the flow-through concept on arrays of open-ended subwavelength holes on suspended gold films.[70] In this case, the open-ended holes were used as nanochannels to transport the solution containing the analyte from one side of the gold film to the other. The advantage of this approach is illustrated in Figure 7.

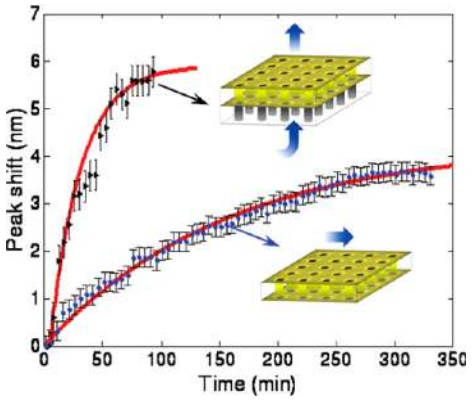

Figure 7. Comparison of the binding curves for the flow-through and the flow-over approaches using arrays of nanoholes in gold thin films. Reprinted with permission from ref 70.

The binding curve ($\Delta\lambda$ vs time) reflects the adsorption of an organic species on the surface of the sensor. The value of $\Delta\lambda$ increases as the surface coverage increases with time, up to a saturation value. The two curves in Figure 7 are for the flow-through experiment and the flow-over (dead-ended holes) arrangement. It is clear that the saturation value is reached much faster in the flow-through case because the small diameter of the holes allows for faster transport to the sensor surface. In principle, a ca. 20 times improvement in the analysis time can be achieved in the flow-through scheme for diffusion-controlled processes. Notice that this advantage is lost when the binding kinetics is no longer controlled by diffusion.[4]

The integration with microfluidics opens the door to the use of fluidic control schemes that can have a direct impact on the performance of the sensor. For instance, although the flow-through nanohole approach, described in Figure 7, has the potential to decrease the time required for chemical analysis, that approach does not provide any direct improvement in the performance metrics, such as sensitivity and LOD. However, the integration of the flow-through nanohole platform in a microfluidic device provides access to fluid manipulation protocols that can lead to lower LODs. This is illustrated in Figure 8, where a scheme of a flow-through sensing element in contact with an electrolyte solution containing a charged analyte (a protein, for instance) is presented.[3] The concentration of the analyte in solution is assumed to be below the LOD. However, a potential bias applied across the perforated nanohole substrate sets up electric-field-induced movements of ions. The electrophoretic (EP) flux of the anions, from both the buffer solution and the analyte, generates a depletion region in the vicinity of the holes that concentrates the analyte of interest. The concentrated analyte plug can then be forced toward the sensor surface using pressure (Figure 8).[3] This combination of electrical and pressure-driven flow has shown to be able to increase the concentration of a protein in the vicinity of the nanohole sensor surface by 100-fold, significantly improving the LOD of the platform.

dx.doi.org/10.1021/la400085r | Langmuir 2013, 29, 5638−5649

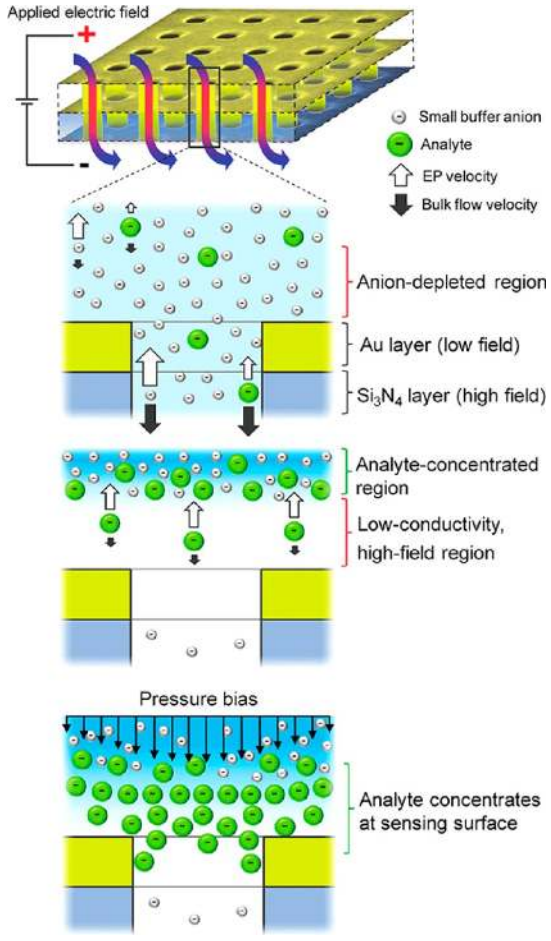

Figure 8. Optofluidic concentration scheme using arrays of flow-through nanoholes. A through-nanohole array in a metallic film immersed in a buffer solution containing a negatively charged analyte of interest is represented. Before the application of an electrical potential bias, the concentrations are the same inside and outside the holes. The application of an appropriate electric field sets up the movement of ions and solvent molecules in a combination of electrophoretic and electroosmotic flows. Because the electric field inside the holes is smaller than everywhere else, the analyte anions end up being accumulated in the vicinity of the holes, creating a depletion region next to the Au layer. A pressure bias is then applied to direct the analyte of interest toward the sensing surface. Reprinted with permission from ref 3.

CONCLUSIONS

Periodic plasmonic structures are promising sensing platforms that combine the regular advantages of SPR (surface-specific label-free sensing) with the possibility of enhanced optical and fluidic integrations. These structures (arrays of nanoholes in metal thin films or arrays of nanoparticles) can now be mass fabricated at low cost by several different approaches, indicating that barriers for their commercialization at competitive prices are no longer a limitation. Several research groups have reported sensor applications using these platforms and have indicated the quality of their sensors by using bulk and surface sensitivities, FoMs, LODs, and the resolution as common performance evaluation parameters. Although the resolution and the LOD appear to be the best parameters for comparing different sensors because they take into account both the sensitivity and the noise, most of the reports quote only sensitivities and FoMs in their performance evaluations. Several novel data acquisitions, data analyses, and experimental implementations have also been reported, leading to further improvements in the performance of the sensors. The Krestchmann–Raether SPR configuration is still the gold standard, although several of the periodic plasmonic platforms have reported comparable performance.

It is clear that pursuing new types of periodic plasmonic sensors will continue to grow, driven by the need for label-free sensing elements in a new generation of microfluidic devices. The advantage of these platforms in terms of miniaturization and multiplexing places them in a unique position to make a significant impact on the next generation of sensor devices, including point-of-care biomedical technologies.

AUTHOR INFORMATION

Notes

The authors declare no competing financial interest.

Biographies

Christina Marshall, photographer, UVic Photo Services

Alexandre G. Brolo obtained his M.Sc. from the University of Sao Paulo (Brazil) and his Ph.D. from the University of Waterloo (Canada). After a postdoctoral tenure at the University of Western Ontario, he joined the University of Victoria as an assistant professor in 2001. Dr. Brolo is now a full professor of chemistry at the University of Victoria, and his current interests are the application of in situ spectroscopic methods to the study of electrochemical systems and the development of plasmonic substrates for enhanced spectroscopy, chemical sensing, nanophotonics, and solar energy conversion.

Jacson De Menezes, photographer

Chiara Valsecchi graduated in chemistry with honors from the University of Milan in 2009. She started to work under the supervision of Prof. Brolo in 2009. Her research is part of the NSERC Strategic

dx.doi.org/10.1021/la400085r | Langmuir 2013, 29, 5638–5649

Network on Bioplasmonic Systems (BiopSys) that aims at the development of a new generation of plasmonic nanosensors for cancer detection. Her role in the project is to optimize the performance of nanohole arrays in gold films and develop an SPR sensing platform for leukemia diagnosis.

■ ACKNOWLEDGMENTS

Our work in plasmonic biosensors is supported by operating grants from the NSERC and the NSERC Strategic Network for Bioplasmonic Systems (BiopSys), Canada. The equipment grant was provided by the Canada Foundation for Innovation (CFI), the British Columbia Knowledge and Development Fund (BCKDF), and the University of Victoria through the New Opportunities Program.

■ REFERENCES

(1) Homola, J. *Surface Plasmon Based Sensors*; Springer Series on Chemical Sensors and Biosensors; Springer-Verlag: Berlin, 2006.
(2) Wijaya, E.; Lenaerts, C.; Maricot, S.; Hastanin, J.; Habraken, S.; Vilcot, J.-P.; Boukherroub, R.; Szunerits, S. Surface plasmon resonance-based biosensors: from the development of different SPR structures to novel surface functionalization strategies. *Curr. Opin. Solid State Mater. Sci.* **2011**, *15*, 208−224.
(3) Escobedo, C.; Brolo, A. G.; Gordon, R.; Sinton, D. Optofluidic concentration: plasmonic nanostructure as concentrator and sensor. *Nano Lett.* **2012**, *12*, 1592−1596.
(4) Escobedo, C.; Brolo, A. G.; Gordon, R.; Sinton, D. Flow-through vs flow-over: analysis of transport and binding in nanohole array plasmonic biosensors. *Anal. Chem.* **2010**, *82*, 10015−10020.
(5) Lesuffleur, A.; Im, H.; Lindquist, N. C.; Lim, K. S.; Oh, S.-H. Laser-illuminated nanohole arrays for multiplex plasmonic microarray sensing. *Opt. Express* **2008**, *16*, 219−224.
(6) De Leebeeck, A.; Kumar, L. K. S.; de Lange, V.; Sinton, D.; Gordon, R.; Brolo, A. G. On-chip surface-based detection with nanohole arrays. *Anal. Chem.* **2007**, *79*, 4094−4100.
(7) Rooney, P.; Rezaee, A.; Xu, S.; Manifar, T.; Hassanzadeh, A.; Podoprygorina, G.; Bohmer, V.; Rangan, C.; Mittler, S. Control of surface plasmon resonances in dielectrically coated proximate gold nanoparticles immobilized on a substrate. *Phys. Rev. B* **2008**, *77*, 23.
(8) Anker, J. N.; Hall, W. P.; Lyandres, O.; Shah, N. C.; Zhao, J.; Van Duyne, R. P. Biosensing with plasmonic nanosensors. *Nat. Mater.* **2008**, *7*, 442−453.
(9) Gao, Y. K.; Gan, Q. Q.; Xin, Z. M.; Cheng, X. H.; Bartoli, F. J. Plasmonic Mach-Zehnder interferometer for ultrasensitive on-chip biosensing. *ACS Nano* **2011**, *5*, 9836−9844.
(10) Stewart, M. E.; Anderton, C. R.; Thompson, L. B.; Maria, J.; Gray, S. K.; Rogers, J. A.; Nuzzo, R. G. Nanostructured plasmonic sensors. *Chem. Rev.* **2008**, *108*, 494−521.
(11) Dmitriev, A. *Nanoplasmonic Sensors*; Springer: New York, 2012.
(12) Mayer, K. M.; Hafner, J. H. Localized Surface plasmon resonance sensors. *Chem. Rev.* **2011**, *111*, 3828−3857.
(13) Szunerits, S.; Boukherroub, R. Sensing using localised surface plasmon resonance sensors. *Chem. Commun.* **2012**, *48*, 8999−9010.
(14) Zhou, W.; Ma, Y.; Yang, H.; Ding, Y.; Luo, X. A label-free biosensor based on silver nanoparticles array for clinical detection of serum p53 in head and neck squamous cell carcinoma. *Int. J. Nanomed.* **2011**, *6*, 381−386.
(15) Zhou, W.; Odom, T. W. Tunable subradiant lattice plasmons by out-of-plane dipolar interactions. *Nat. Nanotechnol.* **2011**, *6*, 423−427.
(16) Fan, M. K.; Andrade, G. F. S.; Brolo, A. G. A review on the fabrication of substrates for surface enhanced Raman spectroscopy and their applications in analytical chemistry. *Anal. Chim. Acta* **2011**, *693*, 7−25.
(17) Kretschm, E; Raether, H. Plasma resonance emission in solids. *Z. Naturforsch., A: Astrophys., Phys. Phys. Chem.* **1968**, *23*, 615−623.
(18) Correia-Ledo, D.; Gibson, K. F.; Dhawan, A.; Couture, M.; Tuan, V.-D.; Graham, D.; Masson, J.-F. Assessing the location of surface plasmons over nanotriangle and nanohole arrays of different size and periodicity. *J. Phys. Chem. C* **2012**, *116*, 6884−6892.
(19) Genet, C.; Ebbesen, T. W. Light in tiny holes. *Nature* **2007**, *445*, 39−46.
(20) Barnes, W. L.; Dereux, A.; Ebbesen, T. W. Surface plasmon subwavelength optics. *Nature* **2003**, *424*, 824−830.
(21) Kelly, K. L.; Coronado, E.; Zhao, L. L.; Schatz, G. C. The optical properties of metal nanoparticles: the influence of size, shape, and dielectric environment. *J. Phys. Chem. B* **2003**, *107*, 668−677.
(22) Volkert, C. A.; Minor, A. M. Focused ion beam microscopy and micromachining. *MRS Bull.* **2007**, *32*, 389−399.
(23) Vieu, C.; Carcenac, F.; Pépin, A.; Chen, Y.; Mejias, M.; Lebib, A.; Manin-Ferlazzo, L.; Couraud, L.; Launois, H. Electron beam lithography: resolution limits and applications. *Appl. Surf. Sci.* **2000**, *164*, 111−117.
(24) Guzenko, V. A.; Ziegler, J.; Savouchkina, A.; Padeste, C.; David, C. Fabrication of large scale arrays of metallic nanodots by means of high resolution e-beam lithography. *Microelectron. Eng.* **2010**, *88*, 1972−1974.
(25) Henzie, J.; Lee, J.; Lee, M. H.; Hasan, W.; Odom, T. W. Nanofabrication of plasmonic structures*. *Annu. Rev. Phys. Chem.* **2009**, *60*, 147−165.
(26) Im, H.; Lee, S. H.; Wittenberg, N. J.; Johnson, T. W.; Lindquist, N. C.; Nagpal, P.; Norris, D. J.; Oh, S.-H. Template-stripped smooth ag nanohole arrays with silica shells for surface plasmon resonance biosensing. *ACS Nano* **2011**, *5*, 6244−6253.
(27) Yao, J. M.; Stewart, M. E.; Maria, J.; Lee, T. W.; Gray, S. K.; Rogers, J. A.; Nuzzo, R. G. Seeing molecules by eye: surface plasmon resonance imaging at visible wavelengths with high spatial resolution and submonolayer sensitivity. *Angew. Chem., Int. Ed.* **2008**, *47*, 5013−5017.
(28) Odom, T. W.; Love, J. C.; Wolfe, D. B.; Paul, K. E.; Whitesides, G. M. Improved pattern transfer in soft lithography using composite stamps. *Langmuir* **2002**, *18*, 5314−5320.
(29) Chen, J.; Shi, J.; Decanini, D.; Cambril, E.; Chen, Y.; Haghiri-Gosnet, A.-M. Gold nanohole arrays for biochemical sensing fabricated by soft UV nanoimprint lithography. *Microelectron. Eng.* **2009**, *86*, 632−635.
(30) Lee, S. H.; Bantz, K. C.; Lindquist, N. C.; Oh, S.-H.; Haynes, C. L. Self-assembled plasmonic nanohole arrays. *Langmuir* **2009**, *25*, 13685−13693.
(31) Gao, H. W.; Yang, J. C.; Lin, J. Y.; Stuparu, A. D.; Lee, M. H.; Mrksich, M.; Odom, T. W. Using the angle-dependent resonances of molded plasmonic crystals to improve the sensitivities of biosensors. *Nano Lett.* **2010**, *10*, 2549−2554.
(32) Nagpal, P.; Lindquist, N. C.; Oh, S. H.; Norris, D. J. Ultrasmooth patterned metals for plasmonics and metamaterials. *Science* **2009**, *325*, 594−597.
(33) Menezes, J. W.; Ferreira, J.; Santos, M. J. L.; Cescato, L.; Brolo, A. G. Large-area fabrication of periodic arrays of nanoholes in metal films and their application in biosensing and plasmonic-enhanced photovoltaics. *Adv. Funct. Mater.* **2010**, *20*, 3918−3924.
(34) Huntington, M. D.; Odom, T. W. A portable, benchtop photolithography system based on a solid-state light source. *Small* **2011**, *7*, 3144−3147.
(35) Sun, S.; Leggett, G. J. Matching the resolution of electron beam lithography by scanning near-field photolithography. *Nano Lett.* **2004**, *4*, 1381−1384.
(36) Henzie, J.; Lee, M. H.; Odom, T. W. Multiscale patterning of plasmonic metamaterials. *Nat. Nanotechnol.* **2007**, *2*, 549−554.
(37) Menezes, J. W.; Barea, L. A. M.; Chillcce, E. F.; Frateschi, N.; Cescato, L. Comparison of plasmonic arrays of holes recorded by interference lithography and focused ion beam. *Photon. J. IEEE* **2012**, *4*, 544−551.
(38) Shin, D. O.; Jeong, J.-R.; Han, T. H.; Koo, C. M.; Park, H.-J.; Lim, Y. T.; Kim, S. O. A plasmonic biosensor array by block copolymer lithography. *J. Mater. Chem.* **2010**, *20*, 7241−7247.

(39) Lesuffleur, A.; Im, H.; Lindquist, N. C.; Oh, S.-H. Periodic nanohole arrays with shape-enhanced plasmon resonance as real-time biosensors. *Appl. Phys. Lett.* **2007**, *90*, 24.
(40) Homola, J.; Koudela, I.; Yee, S. S. Surface plasmon resonance sensors based on diffraction gratings and prism couplers: sensitivity comparison. *Sens. Actuators, B* **1999**, *54*, 16−24.
(41) Jung, L. S.; Campbell, C. T.; Chinowsky, T. M.; Mar, M. N.; Yee, S. S. Quantitative interpretation of the response of surface plasmon resonance sensors to adsorbed films. *Langmuir* **1998**, *14*, 5636−5648.
(42) Stenberg, E.; Persson, B.; Roos, H.; Urbaniczky, C. Quantitative determination of surface concentration of protein with surface plasmon resonance using radiolabeled proteins. *J. Colloid Interface Sci.* **1991**, *143*, 513−526.
(43) Stewart, M. E.; Yao, J. M.; Maria, J.; Gray, S. K.; Rogers, J. A.; Nuzzo, R. G. Multispectral thin film biosensing and quantitative imaging using 3D plasmonic crystals. *Anal. Chem.* **2009**, *81*, 5980−5989.
(44) Vazquez-Mena, O.; Sannomiya, T.; Villanueva, L. G.; Voros, J.; Brugger, J. Metallic nanodot arrays by stencil lithography for plasmonic biosensing applications. *ACS Nano* **2011**, *5*, 844−853.
(45) Haes, A. J.; Zou, S.; Schatz, G. C.; Van Duyne, R. P. A nanoscale optical biosensor: the long range distance dependence of the localized surface plasmon resonance of noble metal nanoparticles. *J. Phys. Chem. B* **2003**, *108*, 109−116.
(46) Offermans, P.; Schaafsma, M. C.; Rodriguez, S. R. K.; Zhang, Y.; Crego-Calama, M.; Brongersma, S. H.; Rivas, J. G. Universal scaling of the figure of merit of plasmonic sensors. *ACS Nano* **2011**, *5*, 5151−5157.
(47) Bahrami, F.; Alam, M. Z.; Aitchison, J. S.; Mojahedi, M. Dual polarization measurements in the hybrid plasmonic biosensors.*Plasmonics* **2012**, doi: 10.1007/s11468-012-9411-z.
(48) Luk'yanchuk, B.; Zheludev, N. I.; Maier, S. A.; Halas, N. J.; Nordlander, P.; Giessen, H.; Chong, C. T. The Fano resonance in plasmonic nanostructures and metamaterials. *Nat. Mater.* **2010**, *9*, 707−715.
(49) Zhang, S.; Bao, K.; Halas, N. J.; Xu, H.; Nordlander, P. Substrate-induced fano resonances of a plasmonic nanocube: a route to increased-sensitivity localized surface plasmon resonance sensors revealed. *Nano Lett.* **2011**, *11*, 1657−1663.
(50) Yanik, A. A.; Cetin, A. E.; Huang, M.; Artar, A.; Mousavi, S. H.; Khanikaev, A.; Connor, J. H.; Shvets, G.; Altug, H. Seeing protein monolayers with naked eye through plasmonic Fano resonances. *Proc. Natl. Acad. Sci. U.S.A.* **2011**, *108*, 11784−11789.
(51) Escobedo, C.; Vincent, S.; Choudhury, A. I. K.; Campbell, J.; Brolo, A. G.; Sinton, D.; Gordon, R. Integrated nanohole array surface plasmon resonance sensing device using a dual-wavelength source. *J. Micromech. Microeng.* **2011**, *21*, 11.
(52) Zhou, Y.; Xu, H.; Dahlin, A. B.; Vallkil, J.; Borrebaeck, C. A. K.; Wingren, C.; Liedberg, B.; Hook, F. Quantitative interpretation of gold nanoparticle-based bioassays designed for detection of immunocomplex formation. *Biointerphases* **2007**, *2*, 6−15.
(53) M. Das, D. H.; R. Nirwan, A. G.; Brolo, K.; Kavanagh, L.; Gordon, R. Improved performance of nanohole surface plasmon resonance sensors by the integrated response method. *IEEE Photon. J.* **2011**, *3*, 441−449.
(54) Ekgasit, S, T. C.; Yu , F; Knoll, W. Influence of the metal film thickness on the sensitivity of surface plasmon resonance biosensors. *Appl. Spectrosc.* **2005**, *59*, 661−667.
(55) Lee, K.-S.; El-Sayed, M. A. Gold and silver nanoparticles in sensing and imaging: sensitivity of plasmon response to size, shape, and metal composition. *J. Phys. Chem. B* **2006**, *110*, 19220−19225.
(56) Acimovic, S. S.; Kreuzer, M. P.; Gonzalez, M. U.; Quidant, R. Plasmon near-field coupling in metal dimers as a step toward single-molecule sensing. *ACS Nano* **2009**, *3*, 1231−1237.
(57) Eftekhari, F.; Gordon, R.; Ferreira, J.; Brolo, A. G.; Sinton, D. Polarization-dependent sensing of a self-assembled monolayer using biaxial nanohole arrays. *Appl. Phys. Lett.* **2008**, *92*, 253103-3−.
(58) Najiminaini, M.; Vasefi, F.; Kaminska, B.; Carson, J. J. L. Effect of surface plasmon energy matching on the sensing capability of metallic nano-hole arrays. *Appl. Phys. Lett.* **2012**, *100*, 6.
(59) Blanchard-Dionne, A. P.; Guyot, L.; Patskovsky, S.; Gordon, R.; Meunier, M. Intensity based surface plasmon resonance sensor using a nanohole rectangular array. *Opt. Express* **2011**, *19*, 15041−15046.
(60) Fan, H.; Buckley, R.; Berini, P. Passive long-range surface plasmon-polariton devices in Cytop. *Appl. Opt.* **2012**, *51*, 1459−1467.
(61) Wark, A. W.; Lee, H. J.; Corn, R. M. Long-range surface plasmon resonance imaging for bioaffinity sensors. *Anal. Chem.* **2005**, *77*, 3904−3907.
(62) Markowicz, P. P.; Law, W. C.; Baev, A.; Prasad, P. N.; Patskovsky, S.; Kabashin, A. Phase-sensitive time-modulated surface plasmon resonance polarimetry for wide dynamic range biosensing. *Opt. Express* **2007**, *15*, 1745−1754.
(63) Kim, D.-K.; Yoo, S. M.; Park, T. J.; Yoshikawa, H.; Tamiya, E.; Park, J. Y.; Lee, S. Y. Plasmonic properties of the multispot copper-capped nanoparticle array chip and its application to optical biosensors for pathogen detection of multiplex DNAs. *Anal. Chem.* **2011**, *83*, 6215−6222.
(64) Vogel, N.; Jung, M.; Bocchio, N. L.; Retsch, M.; Kreiter, M.; Koeper, I. Reusable localized surface plasmon sensors based on ultrastable nanostructures. *Small* **2010**, *6*, 104−109.
(65) Hicks, E. M.; Zhang, X.; Zou, S.; Lyandres, O.; Spears, K. G.; Schatz, G. C.; Van Duyne, R. P. Plasmonic properties of film over nanowell surfaces fabricated by nanosphere lithography. *J. Phys. Chem. B* **2005**, *109*, 22351−22358.
(66) Cinel, N. A.; Butun, S.; Ozbay, E. Electron beam lithography designed silver nano-disks used as label free nano-biosensors based on localized surface plasmon resonance. *Opt. Express* **2012**, *20*, 2587−2597.
(67) Stark, P. R. H.; Halleck, A. E.; Larson, D. N. Short order nanohole arrays in metals for highly sensitive probing of local indices of refraction as the basis for a highly multiplexed biosensor technology. *Methods* **2005**, *37*, 37−47.
(68) Zhou, W. J.; Halpern, A. R.; Seefeld, T. H.; Corn, R. M. Near infrared surface plasmon resonance phase imaging and nanoparticle-enhanced surface plasmon resonance phase imaging for ultrasensitive protein and DNA biosensing with oligonucleotide and aptamer microarrays. *Anal. Chem.* **2012**, *84*, 440−445.
(69) Piliarik, M.; Vala, M.; Tichy, I.; Homola, J. Compact and low-cost biosensor based on novel approach to spectroscopy of surface plasmons. *Biosens. Bioelectron.* **2009**, *24*, 3430−3435.
(70) Eftekhari, F.; Escobedo, C.; Ferreira, J.; Duan, X. B.; Girotto, E. M.; Brolo, A. G.; Gordon, R.; Sinton, D. Nanoholes as nanochannels: flow-through plasmonic sensing. *Anal. Chem.* **2009**, *81*, 4308−4311.